

Calibration of a productivity model for the microalgae *Dunaliella salina* accounting for light and temperature

Quentin Béchet, Philippe Moussion, Olivier Bernard

► **To cite this version:**

Quentin Béchet, Philippe Moussion, Olivier Bernard. Calibration of a productivity model for the microalgae *Dunaliella salina* accounting for light and temperature. *Algal Research - Biomass, Biofuels and Bioproducts*, Elsevier, 2016, 21, pp.156 - 160. <10.1016/j.algal.2016.11.001>. <hal-01410980>

HAL Id: hal-01410980

<https://hal.inria.fr/hal-01410980>

Submitted on 27 Jan 2017

HAL is a multi-disciplinary open access archive for the deposit and dissemination of scientific research documents, whether they are published or not. The documents may come from teaching and research institutions in France or abroad, or from public or private research centers.

L'archive ouverte pluridisciplinaire **HAL**, est destinée au dépôt et à la diffusion de documents scientifiques de niveau recherche, publiés ou non, émanant des établissements d'enseignement et de recherche français ou étrangers, des laboratoires publics ou privés.



1 Calibration of a productivity model for the microalgae

2 *Dunaliella salina* accounting for light and temperature

3

4 Quentin Béchet^{a,b*}, Philippe Moussion^{a,b}, Olivier Bernard^{a,b}

5

6 ^a Université Côte d'Azur, Inria, BIOCORE, BP 93 06902 Sophia Antipolis Cedex, France

7 ^b Sorbonne Universités, UPMC Université Paris 06, CNRS, UMR 7093, LOV, Observatoire
8 océanologique, F-06230, Villefranche/mer, France

9

10 * Corresponding author

11 Telephone: +33 4 92 38 71 74

12 Fax: + 33 4 92 38 78 58

13 Email: quentin.bechet@inria.fr

14 Abstract

15

16 This study aimed to calibrate a productivity model for the algal species *Dunaliella salina*
17 accounting for the impacts of light intensity and temperature. The calibration was performed
18 by using a dedicated experimental set-up measuring short-term oxygen production rates at
19 different light intensities. The rate of photosynthesis was shown to follow a typical Monod
20 function of light intensity. The slope of Photosynthesis-light curves at low light intensity was
21 also shown to be independent on temperature and the evolution of model parameters with
22 temperature obeyed relationships consistent with previous observations in the literature.
23 Finally, the rate of respiration was shown to follow an Arrhenius function of temperature.
24 This good level of agreement with prior observations in the literature indirectly validates the
25 experimental technique used for model calibration. The resulting model should therefore yield
26 accurate productivity predictions in outdoor cultivation systems.

27

28 Keywords: Algae; *D. salina*; growth kinetics; productivity model; photosynthesis; respiration

29 1. Introduction

30 With the objective to accurately assess the economical and environmental feasibility of full-
31 scale algal cultivation for biofuel production, a large number of studies developed
32 mathematical models predicting algal productivity in outdoor cultivation systems [1–3].
33 These models can be used to improve process design or develop optimization strategies
34 maximizing algal productivity. For instance, Slegers et al. [4] used a mathematical model
35 predicting growth rates of *Phaeodactylum tricornutum* and *Thalassiosira pseudonana* to
36 optimize the design of closed photobioreactors. Similarly, Béchet et al.[5] proposed an
37 optimization strategy based on the dynamic control of pond depth and hydraulic retention
38 time to increase productivity while reducing water demand, using a productivity model for
39 *Chlorella vulgaris*. Alternatively, adapting the algal species to climatic conditions could
40 potentially boost yearly algal productivity, similarly to crop rotation used in traditional
41 agriculture. For example, algal species having low optimal temperatures could be cultivated in
42 colder climates or simply during winter while heat-resistant algal species could be grown in
43 summer when pond temperature reaches higher levels. With the objective to assess the
44 benefits of these 'algal culture rotation' strategies, it is necessary to calibrate algal productivity
45 models for a large number of species. However, while many studies in the literature
46 developed productivity models, these models have been calibrated on a limited number of
47 algal species. In particular, the impact of temperature was often neglected in past studies,
48 which limits models application to outdoor systems where temperature significantly varies
49 [1].

50

51 Within this context, our research group has been developing mathematical models to predict
52 algal productivity in various outdoor cultivation systems from meteorological hourly data,
53 system design and operation. This modeling framework combined models predicting system

54 temperature with a biological model predicting algal productivity as a function of light and
55 temperature. So far, the biological model has only been calibrated for a single algal species,
56 *Chlorella vulgaris* (see Béchet et al. [6]). The objective of this study was therefore to calibrate
57 a productivity model for another algal species, *Dunaliella salina*, this species being the third
58 most cultivated microalgae [7]. *Chlorella vulgaris* and *Dunaliella salina* are both
59 Chlorophyceae and share the same tolerance to high temperatures. The methodology followed
60 in this study was therefore similar to the calibration technique followed by Béchet et al. [6],
61 and also because the model for *C. vulgaris* accurately predicted productivities in indoor
62 (accuracy of +/- 15% over 163 days; Béchet et al. [6]) and outdoor (accuracy of +/- 8.4% over
63 148 days, Béchet et al. [8]) reactors.

64 2. Materials and methods

65 2.1. Algae cultivation conditions and biomass characterization

66 The Chlorophyceae *Dunaliella salina* (CCAP 19/18) was cultivated in a cylindrical
67 photobioreactor (diameter: 0.19 m; height: 0.41 m; culture volume: 10 L; gas phase volume:
68 1.6 L). The reactor was illuminated by two metal halide lamps (Osram Powerstar HQI-TS,
69 150W NDL, Neutralweiss de Luxe) providing a light intensity of 1440 $\mu\text{mol}/\text{m}^2\text{-s}$ (measured
70 when the reactor was filled with water with a QSL-2100 PAR scalar irradiance sensor,
71 Biospherical Instruments). Temperature was maintained at 30°C by re-circulating
72 temperature-controlled water in a jacket around the reactor. The reactor was inoculated with a
73 culture of *D. salina* (inoculum volume of approximately 500 mL) grown in axenic conditions
74 (light intensity: 300 $\mu\text{mol}/\text{m}^2\text{-s}$, light-dark cycle: 12:12, temperature: 27°C) and was then
75 operated as a fed-batch system: 9L of solution was replaced every week with fresh f/2
76 medium [9] enriched in phosphorus and nitrogen to ensure that algal growth was not limited
77 by nutrients (Total N and P concentrations in enriched medium: 0.22 g N-NO₃⁻/L; 0.020 g P-

78 PO_3^-/L). Air enriched in CO_2 (2% CO_2) was continuously bubbled in the photobioreactor to
79 ensure that CO_2 supply did not limit algal growth and also to control pH between 7 and 7.5.
80 Algae used for model calibration were extracted from the photobioreactor 2-3 days after
81 medium change during the light-limited growth phase. The biomass concentration in the
82 solution used during model calibration was measured by dry weight [10]. Glass-fiber filters
83 (GF/C, Whatman, diameter: 25mm, No 1822-025) were first dried for several days at 60°C
84 before being weighed. A known volume of the algal solution was then filtered; filters were
85 then rinsed with Ammonium formate (30 g/L) to remove salt. Filters were then dried for 24
86 hours at 60°C before being weighed again. Dry weight concentration was measured in
87 duplicates.

88

89 2.2. Productivity model description

90 Algal productivity (P_{net} , in $\text{kg O}_2/\text{s}$) was expressed as the difference between the gross rate of
91 photosynthesis (P , in $\text{kg O}_2/\text{s}$) and the rate of endogenous respiration (ER , in $\text{kg O}_2/\text{s}$) [6]:

$$92 P_{net} = P - ER \quad (1)$$

93 The gross rate of photosynthesis was expressed as a function of light intensity and
94 temperature by using a 'type-II model' as recommended by Béchet et al. [1]. This type of
95 models is based on the assumption that the local rate of photosynthesis of single algal cells
96 can be expressed as a direct function of the local light intensity cells are exposed to. Béchet et
97 al. [6] used different formulas to express local rates of photosynthesis as a function of local
98 light intensity and showed that the three formulas most commonly used in the literature all
99 satisfyingly fit experimental data. The authors finally selected the Monod formula, as this
100 expression was the most commonly found in literature. The gross rate of photosynthesis was
101 therefore expressed as [6]:

102
$$P_{net} = \int_V P_m(T) \frac{\sigma_X I_{loc}}{K(T) + \sigma_X I_{loc}} X \cdot dV \quad (2)$$

103 where P_m is the maximum specific rate of photosynthesis (kg O₂/kg-s), T is the culture
 104 temperature (°C), K is the half-saturation constant (W/kg), σ_X is the extinction coefficient
 105 (m²/kg), I_{loc} is the local light intensity (W/m², as photosynthetically active radiation or PAR),
 106 X is the algal concentration (kg/m³) and V is the culture volume (m³). The local light intensity
 107 I_{loc} was expressed by using a Beer-Lambert law:

108
$$I_{loc}(l) = I_0 \exp(-\sigma_X X l) \quad (3)$$

109 where l is the light path between the considered location and the reactor external surface (m)
 110 and I_0 is the incident light intensity (W/m²). The evolution of P_m and K with temperature was
 111 fitted to the theoretical model of Bernard and Rémond [11] as this model was shown to
 112 satisfyingly fit the evolution of the specific growth rate of 15 algal species. P_m and K were
 113 therefore expressed as follows:

114
$$p = \begin{cases} \alpha \frac{(T-T_{max})(T-T_{min})^2}{(T_{opt}-T_{min})(T_{opt}-T_{min})(T-T_{opt})-(T_{opt}-T_{max})(T_{opt}+T_{min}-2T)} & \text{if } T_{min} \leq T \leq T_{max} \\ 0 & \text{otherwise} \end{cases} \quad (4)$$

115 where p represents either P_m or K , α is the maximum value of P_m or K , and T_{min} , T_{max} and T_{opt}
 116 are the minimum, maximum, and optimum temperatures for photosynthesis (°C), respectively.

117 The rate of endogenous respiration was expressed using a first-order law:

118
$$ER = \lambda(T) X V \quad (5)$$

119 where λ is the specific respiration rate (kg O₂/kg-s). Several studies showed that the rate of
 120 respiration was an exponential function of temperature [12–14]. The parameter λ was
 121 therefore expressed as follows:

122
$$\lambda(T) = \lambda_0 \exp(\beta T) \quad (6)$$

123 where λ_0 (kg O₂/kg-s⁻¹) and β (°C⁻¹) are determined experimentally.

124

125 2.3. Device used for model calibration

126 The device used for calibration was composed of six cylindrical glass reactors (diameter: 3.48
127 cm; height: 5.82 cm; volume: 55.2 mL) all equipped with an oxygen electrode (Model DO50-
128 GS, Hach) measuring both dissolved oxygen and medium temperature. Each reactor was
129 positioned over a LED lamp (12V PHILIPS EnduraLED 10W MR16 Dimmable 4000 K)
130 which light intensity was independently controlled. A typical experiment consisted on
131 measuring first oxygen production rates when algae were exposed to light (light-phase) and
132 then respiration rates when algae were in the dark (dark phase). These measurements were
133 performed for six different light intensities (range: 0-460 W/m², as PAR) and under constant
134 temperature (see [6] for a complete description of the oxygen measurements). These
135 experiments were then repeated for 6 different temperatures (3.73°C; 10.2°C; 19.7°C, 27.7°C,
136 34.7°C; 40.9°C). Temperature was maintained constant (within approximately +/- 1°C) during
137 the entire duration of the experiment by circulating temperature-controlled air around the
138 reactors. The light intensity reaching the external surface of each reactor was measured by
139 actinometry (see S1 for details). The parameters P_m and K for each temperature were
140 determined by least-square fitting using the *lsqcurvefit* Matlab function. Respiration rates
141 during the dark periods were found to be independent on the light intensity cells where
142 exposed to during the light phase and the parameter λ was determined from the average
143 respiration rate in the six reactors. The parameters T_{min} , T_{max} , T_{opt} , were obtained by least-
144 square fitting (using the *lsqcurvefit* Matlab function) and the parameters λ_0 and β were
145 estimated by log-linear regression. Algae were found to be photosynthetically inactive after
146 exposure to 43°C for 30 min (unpublished data). P_m was therefore considered null at 43°C
147 when determining T_{min} , T_{max} , and T_{opt} . Based on the linear relationship between P_m and K (see
148 section 3.1 for details), K was also assumed null at this temperature.

149

150 2.4. Measurement of extinction coefficient

151 The extinction coefficient σ_X was experimentally determined by measuring the light
152 intensities entering and exiting the reactors for different algal concentrations (see S2 for
153 details). Similarly to the formula proposed by [15], the extinction coefficient was expressed as
154 follows:

$$155 \sigma_X = AX^B \quad (7)$$

156 where A and B are empirical coefficients ($A = 79.1$; $B = -0.37$, see S2 for details). The
157 dependence of the extinction coefficient on algal concentration was mostly due to light
158 scattering by algal cells. Scattered photons indeed exited the reactors through the lateral side
159 of the reactors. This effect was reinforced by the fact that LEDs lamps did not emit light in a
160 vertical direction but in a cone of an angle 30° , which increases the fraction of light lost
161 through the reactors lateral sides. When the algal concentration increased, most of photons
162 were absorbed by algal cells and the fraction of light exiting the reactors through the lateral
163 sides decreased. This explains why the extinction coefficient is less sensitive to X for high
164 algal concentrations (Equation 7; see S2 for further detail). Calibration experiments were
165 therefore performed at relatively high algal concentrations to ensure that most of incoming
166 light was absorbed by algae.

167

168 2.5. Application to the calibration device

169 Based on Equations 1-7, the algal productivity in each reactor used for model calibration was
170 expressed as follows:

$$171 P_{net}(T, I_0) = \frac{P_m(T)S}{\sigma_X} \ln \left(\frac{K(T) + \sigma_X I_0}{K(T) + \sigma_X I_0 \cdot \exp(-\sigma_X XL)} \right) - \lambda(T)XSL \quad (8)$$

172 where T is the culture temperature ($^\circ\text{C}$), I_0 is the incident light intensity at the reactor bottom
173 (W m^{-2}), P_m , K and λ are the temperature-dependent model parameters (see Equations 4 and

174 6), σ_X is the extinction coefficient (see Equation 7), X is the algal concentration (kg m^{-3}), and
175 L and S are the reactor height (m) and section surface area (m^2), respectively.

176

177 2.6. Monte-Carlo simulations

178 Monte-Carlo simulations were performed to quantify the impact of experimental error on the
179 fitted values of model parameters P_m , K and λ . Namely, four key measurements were found to
180 have a significant impact on model parameters:

- 181 - The extinction coefficient σ_X : coefficients A and B in Equation 7 were found to vary in
182 the ranges 74.50-82.78 and -0.20--0.48, respectively (see S2 for details);
- 183 - The dissolved oxygen concentration: oxygen probes were found to be accurate at +/-
184 4.7% (see S3 for details);
- 185 - The incident light intensity I_0 : Measurements by actinometry were assumed to be
186 accurate at +/-10% based on the study of Hatchard and Parker [16] (See S1 for
187 details).
- 188 - The algal concentration X : an accuracy of +/-7% on dry weight measurements was
189 assumed by analogy with the study of Béchet et al. [6].

190

191 In practice, the uncertainties on the parameters P_m , K and λ were obtained from the following
192 Monte-Carlo approach. Assuming that errors were normally distributed, a large artificial data
193 set was generated by adding a normally distributed error to the measurements (algal
194 concentration X , light intensity I_0 and oxygen concentration) and the extinction coefficient
195 (σ_X). A total of 2000 artificial data sets were thus generated and the parameters P_m , K and λ
196 were determined with a minimization algorithm for each data set. This approach yielded a
197 normal distribution for P_m , K and λ , which allowed determining confidence intervals for each
198 of these parameters. These resulting confidence intervals were then used to determine levels

199 of uncertainty on the parameters T_{min} , T_{max} , T_{opt} , λ_0 and β through another set of Monte-Carlo
200 simulations (see [6] for further details on Monte-Carlo simulations).

201

202 2.7. Conversion coefficients from oxygen to biomass productivity

203 The productivity model developed in this study predicts algal productivity in terms of oxygen
204 (see Equations 1-6). For engineering purposes, it is however necessary to express
205 productivities in terms of biomass. The conversion from oxygen to biomass productivities
206 was performed by following the approach of Béchet et al. [6]. This conversion was based on
207 the assumption of a photosynthetic quotient of 1 mole of CO₂ consumed for the production of
208 1 mole of O₂ during the light reactions of photosynthesis, which was supported by the
209 experimental measurement of the photosynthetic quotient of a close algal species (*Dunaliella*
210 *tertiolecta*) by Wegmann and Metzner [17]. This photosynthetic quotient of 1 does not
211 include respiratory mechanisms and only reflects photosynthesis. From the knowledge of
212 algal composition and by considering that nitrate was used as a nitrogen source, the following
213 conversion coefficients were obtained (see S4 for details):

214 - $P_m' [\text{kg/kg-s}] = 0.75 (\pm 0.10) P_m [\text{kg O}_2/\text{kg-s}]$

215 - $\lambda' [\text{kg/kg-s}] = 0.75 (\pm 0.10) \lambda [\text{kg O}_2/\text{kg-s}]$ at daytime

216 - $\lambda' [\text{kg/kg-s}] = 0.9375 (\pm 0.10) \lambda [\text{kg O}_2/\text{kg-s}]$ at nighttime

217

218 3. Results and discussion

219 3.1. Rate of photosynthesis

220 Figure 1 shows that the Type-II model coupling a Monod formula with the modified Beer-
221 Lambert law was able to describe the evolution of the rate of photosynthesis with light
222 intensity. These PI-curves do not exhibit the typical decrease at high light intensities due to

223 photo-inhibition observed for *D. salina* in dilute cultures through chlorophyll fluorescence
224 measurements by Combe et al. [18]. This is explained by the high algal concentration that
225 ensured that only a small fraction of cells were photo-inhibited, so that the impact of photo-
226 inhibition was minimal, as suggested by Bernard [19]. Experimental errors caused relatively
227 high uncertainty on fitted values of P_m and K as shown in Table 1 and especially at the
228 temperature of 40.9°C as the gross productivity was only measured at two light intensities (the
229 oxygen net productivity was negative at low light intensities due to high respiration rates at
230 this temperature, and oxygen concentration remained null during all experiment). Because of
231 these experimental uncertainties, it was difficult to accurately identify P_m and K separately. In
232 other words, various combinations of P_m and K could yield equally satisfying fits in Figure 1.
233 In spite of these levels of inaccuracy, Figure 2 shows that P_m and K were correlated ($R^2 =$
234 0.87558), which was previously observed by Béchet et al. [6]. The ratio P_m/K indeed
235 represents the maximum 'yield' of photosynthesis (in kg O₂/W-s), i.e. the amount of oxygen
236 produced through photosynthesis per unit light energy captured by cells. For low light
237 intensities, this maximum yield is theoretically independent of temperature [20], which
238 explains the linearity observed in Figure 2.

239

240 Figure 3 shows that experimental values of P_m followed a typical response to temperature
241 characterized by a slow increase from cold to optimal temperatures before a fast drop for
242 higher temperatures. The model of Bernard and Rémond [11] especially developed for this
243 type of temperature response thus provides a good fit to experimental data (Figure 3).

244 Interestingly, the model of Bernard and Rémond successfully described the evolution of K ,
245 with similar values for T_{min} , T_{max} , and T_{opt} as shown in Table 2. This similarity is explained by
246 the linearity between P_m and K shown in Figure 2. The values of T_{min} , T_{opt} and T_{max} are within
247 the range of values obtained by Bernard and Rémond [11] for 15 other algal species. The

248 value of the maximum temperature T_{max} is in the upper range of reported values for other algal
249 species, which may be explained by two reasons. Firstly, *D. salina* is known to resist to high
250 temperatures as this species is naturally found in shallow water bodies in which temperature
251 can reach relatively high values [21,22]. In addition, this model calibration is based on short-
252 term measurements of photosynthesis (approximately 30 min) while Bernard and Rémond
253 [11] fitted their model on growth rate measurements obtained over several days of cultivation.
254 Even if Bernard and Rémond [11] did not calibrate their model on *D. salina* data, this
255 difference in time scales may explain the relatively high T_{max} value (43°C) as short-term and
256 long-term algal responses are not controlled by the same biological processes. Oxygen
257 production indeed reflects the rate of initial non-enzymatic steps of photosynthesis (usually
258 referred to as "light reactions"), while carbon fixation through Calvin cycle and more
259 generally growth involve enzymatic processes that are more impacted by temperatures. For
260 example, Béchet et al. [6] showed that *Chlorella vulgaris* was unable to sustain growth at a
261 constant temperature of 35°C for more than 1-2 hours while the oxygen productivity peaked at
262 38°C. The uncertainty on P_m and K showed in Table 1 caused levels of uncertainty on T_{max} ,
263 T_{min} and T_{opt} similar to the confidence intervals presented by Bernard and Rémond [11], even
264 if methods for uncertainty estimations were based on different approaches (Table 2).

265

266 3.2. Respiration rate

267 Figure 4 shows that the specific respiration rate increased exponentially with temperature over
268 the range of temperatures tested. Similar observations were reported for a large number of
269 algal species as reviewed by Robarts and Zohary [23]. Based on the values reported in Table
270 1, the coefficients λ_0 and β (with corresponding confidence intervals at 95%) were $6.45 \cdot 10^{-7}$
271 ($\pm 0.34 \cdot 10^{-7}$) s^{-1} and 0.0715 (± 0.0002) $^{\circ}C^{-1}$, respectively.

272

273 4. Conclusions

274 The results obtained during the model calibration performed on *D. salina* are consistent with
275 prior observations in the literature, namely:

- 276 - The rate of gross oxygen productivity followed a typical Monod-like response to light
277 intensity;
- 278 - The maximum specific rate of oxygen production was linearly correlated to the half-
279 saturation constant of the Monod model, indicating that oxygen production efficiency
280 is as expected independent of temperature at low light intensities;
- 281 - The evolutions of the maximum specific rate of photosynthesis and half-saturation
282 constant with temperature satisfyingly fitted Bernard and Rémond's model.
- 283 - Respiration rates were shown to increase exponentially with temperature, which is
284 consistent with prior observations in the literature.
- 285 - These results also confirm that *Dunaliella salina* can grow in a relatively wide
286 temperature range and resist to relatively high temperatures.

287 These results indicate that the experimental technique used for model calibration is valid
288 and that the productivity model should yield accurate predictions in outdoor cultivation
289 systems.

290

291

292

293 Acknowledgments:

294 The authors are grateful for the support of the ANR-13-BIME-004 Purple Sun and the
295 Inria Project Lab *Algae in silico*. Margaux Caïa (Inria BIOCORE/LOV) is acknowledged
296 for early work on the device used for model calibration.

297

298 References

- 299 [1] Q. Béchet, A. Shilton, B. Guieysse, Modeling the effects of light and temperature on
300 algae growth: State of the art and critical assessment for productivity prediction during
301 outdoor cultivation, *Biotechnol. Adv.* 31 (2013) 1648–1663.
- 302 [2] E. Lee, M. Jalalizadeh, Q. Zhang, Growth kinetic models for microalgae cultivation: A
303 review, *Algal Res.* 12 (2015) 497–512. doi:10.1016/j.algal.2015.10.004.
- 304 [3] O. Bernard, F. Mairet, B. Chachuat, Modelling of Microalgae Culture Systems with
305 Applications to Control and Optimization, in: C. Posten, S. Feng Chen (Eds.),
306 *Microalgae Biotechnol.*, Springer International Publishing, Cham, 2016: pp. 59–87.
307 doi:10.1007/10_2014_287.
- 308 [4] P.M. Slegers, P.J.M. van Beveren, R.H. Wijffels, G. Van Straten, A.J.B. van Boxtel,
309 Scenario analysis of large scale algae production in tubular photobioreactors, *Appl.*
310 *Energy.* 105 (2013) 395–406. doi:10.1016/j.apenergy.2012.12.068.
- 311 [5] Q. Béchet, A. Shilton, B. Guieysse, Maximizing Productivity and Reducing
312 Environmental Impacts of Full-Scale Algal Production through Optimization of Open
313 Pond Depth and Hydraulic Retention Time, *Environ. Sci. Technol.* (2016)
314 *acs.est.5b05412.* doi:10.1021/acs.est.5b05412.
- 315 [6] Q. Béchet, P. Chambonnière, A. Shilton, G. Guizard, B. Guieysse, Algal productivity
316 modeling: A step toward accurate assessments of full-scale algal cultivation,
317 *Biotechnol. Bioeng.* 112 (2015) 987–996. doi:10.1002/bit.25517.
- 318 [7] J. Benemann, Microalgae for biofuels and animal feeds, *Energies.* 6 (2013) 5869–5886.
319 doi:10.3390/en6115869.
- 320 [8] Q. Béchet, A. Shilton, B. Guieysse, Full-scale validation of a model of algal
321 productivity, *Environ. Sci. Technol.* 48 (2014) 13826–13833.
- 322 [9] R.R.L. Guillard, J.H. Ryther, Studies of marine planktonic diatoms: I. *Cyclotella Nana*

- 323 Hustedt and *Denotula Confervacea* (CLEVE) Gran., *Can. J. Microbiol.* 8 (1962) 229–
324 239. doi:10.1139/m62-029.
- 325 [10] C.J. Zhu, Y.K. Lee, Determination of biomass dry weight of marine microalgae, *J.*
326 *Appl. Phycol.* 9 (1997) 189–194. doi:10.1023/A:1007914806640.
- 327 [11] O. Bernard, B. Rémond, Bioresource Technology Validation of a simple model
328 accounting for light and temperature effect on microalgal growth, *Bioresour. Technol.*
329 123 (2012) 520–527. doi:10.1016/j.biortech.2012.07.022.
- 330 [12] C.D. Collins, C.W. Boylen, Physiological responses of *Anabaena variabilis*
331 (*Cyanophyceae*) to instantaneous exposure to various combinations of light intensity
332 and temperature, *J. Phycol.* 18 (1982) 206–211.
- 333 [13] J.U. Grobbelaar, C.J. Soeder, Respiration losses in planktonic green algae cultivated in
334 raceway ponds, *J. Plankton Res.* 7 (1985) 497–506. doi:10.1093/plankt/7.4.497.
- 335 [14] F. Le Borgne, J. Pruvost, Investigation and modeling of biomass decay rate in the dark
336 and its potential influence on net productivity of solar photobioreactors for microalga
337 *Chlamydomonas reinhardtii* and cyanobacterium *Arthrospira platensis*, *Bioresour.*
338 *Technol.* 138 (2013) 271–276. doi:10.1016/j.biortech.2013.03.056.
- 339 [15] A. Morel, Optical modeling of the upper ocean in relation to its biogenous matter
340 content (case I waters), *J. Geophys. Res.* 93 (1988) 10749–10768.
341 doi:10.1029/JC093iC09p10749.
- 342 [16] C.G. Hatchard, C.A. Parker, A New Sensitive Chemical Actinometer. II. Potassium
343 Ferrioxalate as a Standard Chemical Actinometer, *Proc. R. Soc. London A Math. Phys.*
344 *Eng. Sci.* 235 (1956) 518–536.
345 <http://rspa.royalsocietypublishing.org/content/235/1203/518.abstract>.
- 346 [17] K. Wegmann, H. Metzner, Synchronization of *Dunaliella* cultures, *Arch. Mikrobiol.* 78
347 (1971) 360–367. doi:10.1007/BF00412276.

- 348 [18] C. Combe, P. Hartmann, S. Rabouille, A. Talec, O. Bernard, A. Sciandra, Long-term
349 adaptive response to high-frequency light signals in the unicellular photosynthetic
350 eukaryote *Dunaliella salina*, *Biotechnol. Bioeng.* 112 (2015) 1111–1121.
- 351 [19] O. Bernard, Hurdles and challenges for modelling and control of microalgae for CO₂
352 mitigation and biofuel production, *J. Process Control.* 21 (2011) 1378–1389.
353 doi:10.1016/j.jprocont.2011.07.012.
- 354 [20] I.R. Davison, Environmental effects on algal photosynthesis: temperature, *J. Phycol.* 27
355 (1991) 2–8. doi:10.1111/j.0022-3646.1991.00002.x.
- 356 [21] L.J. Borowitzka, M.A. Borowitzka, Commercial Production of β -carotene by
357 *Dunaliella salina* in open ponds, *Bull. Mar. Sci.* 47 (1990) 244–252.
- 358 [22] P.I. Gómez, M.A. González, The effect of temperature and irradiance on the growth
359 and carotenogenic capacity of seven strains of *Dunaliella salina* (Chlorophyta)
360 cultivated under laboratory conditions, *Biol. Res.* 38 (2005) 151–162.
- 361 [23] R.D. Robarts, T. Zohary, Temperature effects on photosynthetic capacity, respiration,
362 and growth rates of bloom-forming cyanobacteria, *New Zeal. J. Mar. Freshw. Res.* 21
363 (1987) 391–399. doi:10.1080/00288330.1987.9516235.
- 364

365 Table 1: Model parameters values at different temperatures (values in parenthesis indicate
 366 confidence level at 95% estimated through Monte-Carlo simulations). Values of P_m and λ in
 367 kg/kg-s can be obtained by using the conversion coefficients provided in Section 2.6. Values
 368 of K can be obtained in $\mu\text{mol/kg-s}$ by using a conversion factor of $4.79 \mu\text{mol/W-s}$ (based on
 369 the spectral distribution of device lamps shown in S1).

Temperature (°C)	3.7	10.2	19.7	27.7	34.7	40.9
P_m (10^{-4} kg O ₂ /kg-s)	0.165 (0.014)	0.571 (0.096)	1.19 (0.25)	2.08 (0.43)	1.77 (0.33)	1.35 (0.88)
K (10^4 W/kg)	0.479 (0.095)	2.46 (0.64)	2.79 (0.87)	4.77 (1.34)	3.34 (0.89)	3.28 (3.31)
λ (10^{-6} kg O ₂ /kg-s)	0.88 (0.05)	1.22 (0.06)	2.55 (0.13)	5.45 (0.28)	7.53 (0.39)	11.5 (0.6)

370

371 Table 2: Bernard and Rémond's model parameters for P_m and K (values in parenthesis indicate
 372 confidence interval at 95% estimated through Monte-Carlo simulations) - Symbols are
 373 defined in Equation 4. Values of α for K can be obtained in $\mu\text{mol}/\text{kg}\cdot\text{s}$ by using a conversion
 374 factor of $4.79 \mu\text{mol}/\text{W}\cdot\text{s}$

Parameter (unit)	T_{min} ($^{\circ}\text{C}$)	T_{opt} ($^{\circ}\text{C}$)	T_{max} ($^{\circ}\text{C}$)	α
P_m (kg O ₂ /kg-s)	-7.8 (8.4)	34.0 (3.9)	43.0 (0.1)	$2.08 \cdot 10^{-4}$ kg O ₂ /kg-s
K (W/kg)	-15.4 (17.3)	33.7 (8.0)	43.0 (0.4)	$4.77 \cdot 10^4$ W/kg

375

376 Figures

377

378 Figure 1: Gross rate of photosynthesis vs. incident light intensity at different temperatures

379 (dots: experimental data; plain lines: theoretical fitting) - Error bars represent standard

380 deviation of error caused by experimental error. Light intensities in W/m^2 can be converted

381 into $\mu\text{mol}/\text{m}^2\text{-s}$ by using a conversion factor of $4.79 \mu\text{mol}/\text{W}\text{-s}$.

382

383 Figure 2: Values of the maximum specific growth rate P_m vs. the half-constant K (dots:

384 experimental data; plain line: linear regression) - Error bars indicate the standard deviation

385 estimated through Monte-Carlo simulations.

386

387 Figure 3: Evolution of the maximum specific oxygen productivity and half-saturation constant

388 with temperature (dots: experimental data; plain line: fitting with Bernard and Rémond's

389 model) - Error bars represent the standard deviation estimated through Monte-Carlo

390 simulations. Values of K can be obtained in $\mu\text{mol}/\text{kg}\text{-s}$ by using a conversion factor of 4.79

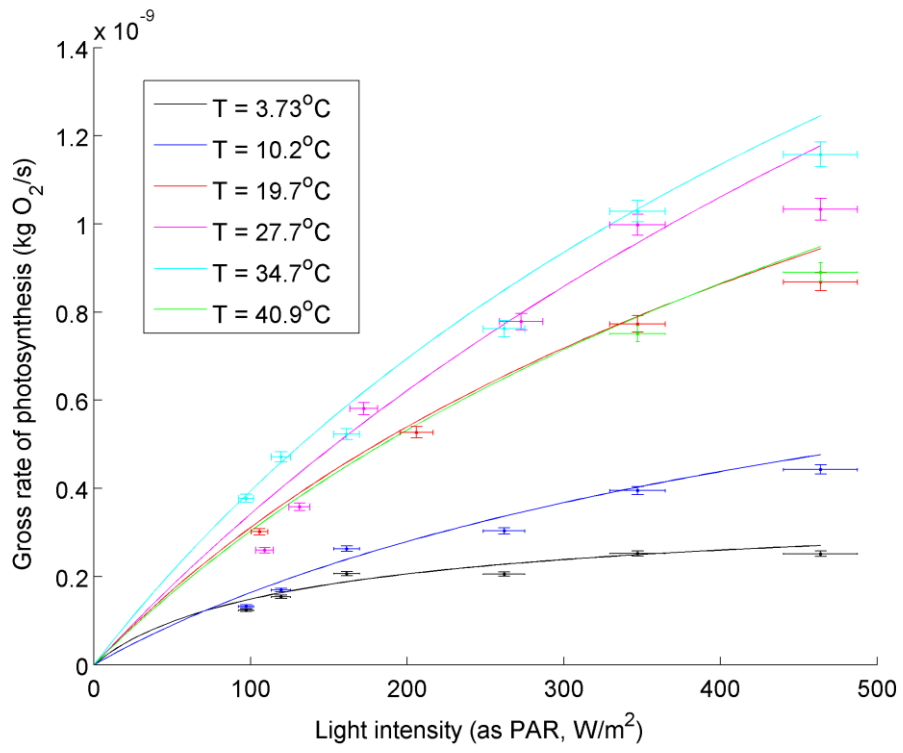
391 $\mu\text{mol}/\text{W}\text{-s}$.

392

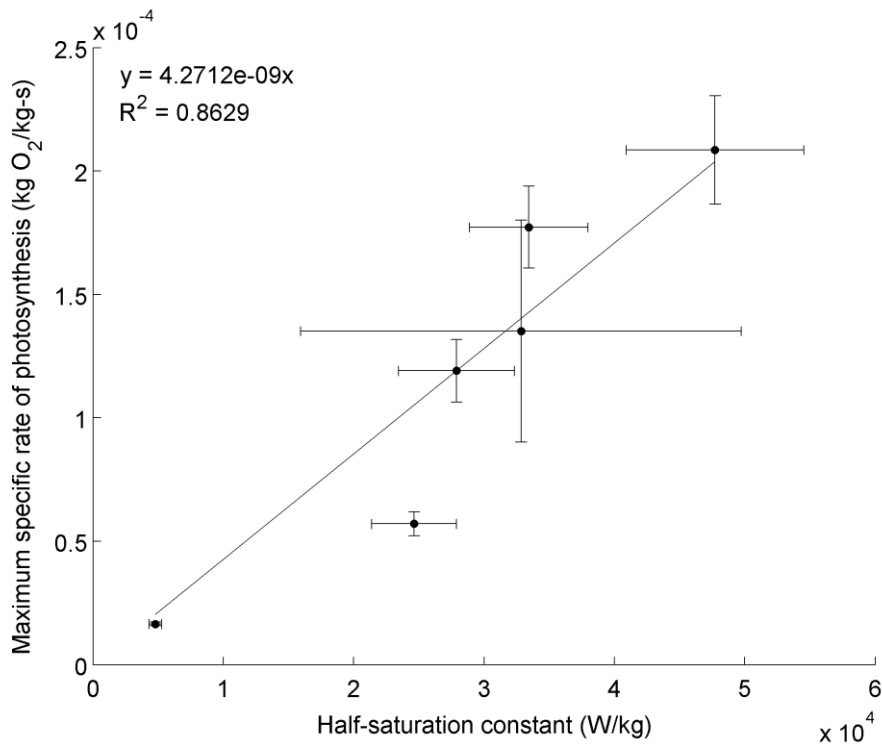
393 Figure 4: Evolution of the respiration specific rate with temperature (dots: experimental data;

394 plain line: fitting to an exponential function as described by Equation 6) - Error bars represent

395 standard deviation estimated through Monte-Carlo simulations.

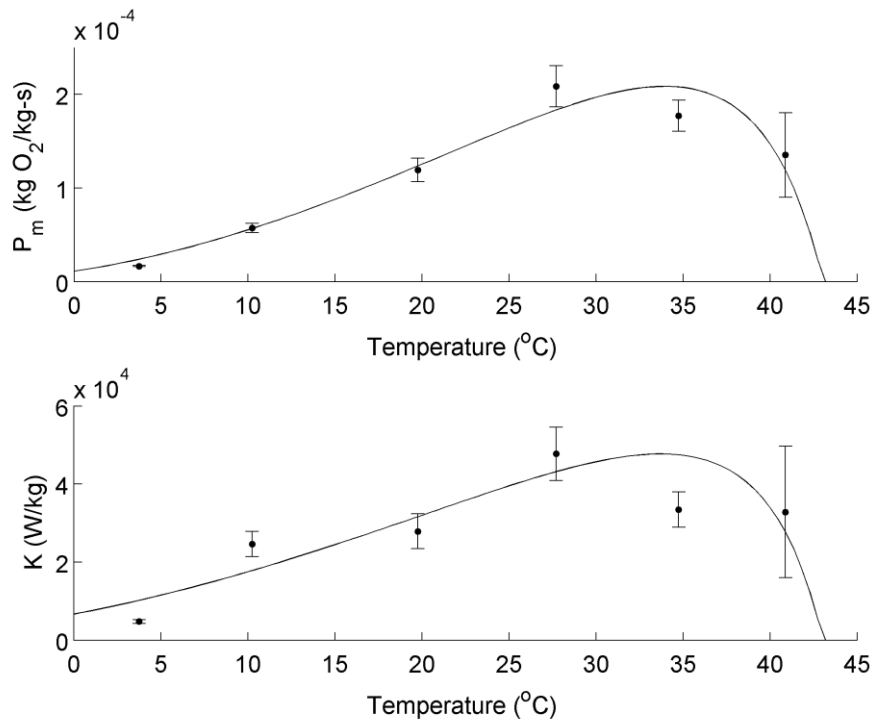


398 Figure 2



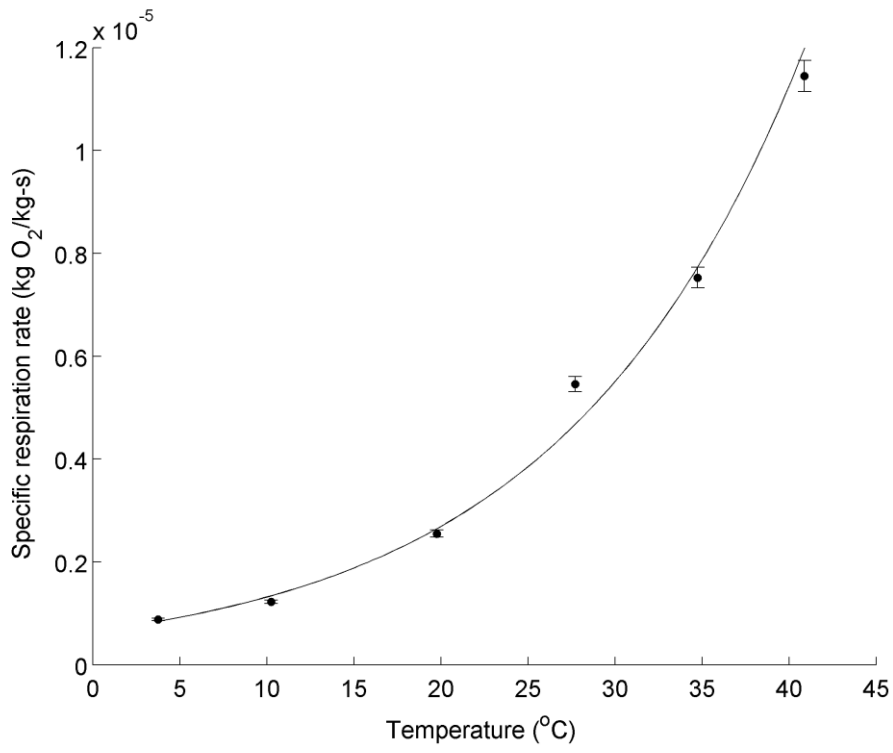
399

400 Figure 3



401

402 Figure 4



403